THE PROTEIN SOCIETY

Structural basis for tankyrase-RNF146 interaction reveals noncanonical tankyrase-binding motifs

Paul A. DaRosa,[1,2] Rachel E. Klevit,[1]* and Wenqing Xu[2]*

[1]Department of Biochemistry, University of Washington, Seattle, Washington 98195
[2]Department of Biological Structure, University of Washington, Seattle, Washington 98195

Received 15 January 2018; Accepted 26 March 2018
DOI: 10.1002/pro.3413
Published online 31 March 2018 proteinscience.org

Abstract: Poly(ADP-ribosyl)ation (PARylation) catalyzed by the tankyrase enzymes (Tankyrase-1 and -2; a.k.a. PARP-5a and -5b) is involved in mitosis, telomere length regulation, GLUT-4 vesicle transport, and cell growth and differentiation. Together with the E3 ubiquitin ligase RNF146 (a.k.a. Iduna), tankyrases regulate the cellular levels of several important proteins including Axin, 3BP2, and angiomotins, which are key regulators of Wnt, Src and Hippo signaling, respectively. These tankyrase substrates are first PARylated and then ubiquitylated by RNF146, which is allosterically activated by binding to PAR polymer. Each tankyrase substrate is recognized by a tankyrase-binding motif (TBM). Here we show that RNF146 binds directly to tankyrases via motifs in its C-terminal region. Four of these RNF146 motifs represent novel, extended TBMs, that have one or two additional amino acids between the most conserved Arg and Gly residues. The individual RNF146 motifs display weak binding, but together mediate a strong multivalent interaction with the substrate-binding region of TNKS, forming a robust one-to-one complex. A crystal structure of the first RNF146 noncanonical TBM in complex with the second ankyrin repeat domain of TNKS shows how an extended motif can be accommodated in a peptide-binding groove on tankyrases. Overall, our work demonstrates the existence of a new class of extended TBMs that exist in previously uncharacterized tankyrase-binding proteins including those of IF4A1 and NELFE.

Keywords: tankyrase; TNKS; RNF146; PARylation; IF4A1; NELFE; tankyrase-binding motif; Wnt

Abbreviations: PAR, poly-ADP-ribose; TNKS, tankyrase or tankyrase 1

Additional Supporting Information may be found in the online version of this article.

Significance: The RNF146-tankyrase axis regulates the degradation of many important proteins implicated in disease such as Axin and 3BP2, but the direct interaction between RNF146 and tankyrase has not been characterized. Here we show the structural basis for the RNF146-TNKS interaction and find that RNF146 binds to tankyrase via the simultaneous engagement of multiple short motifs. Our structural data define a new class of tankyrase-binding motifs that we show exists in previously uncharacterized tankyrase binders.

Grant sponsor: the Director, Office of Science, Office of Basic Energy Sciences, of the U.S. Department of Energy; Grant number: DE-AC02-05CH11231; Grant sponsor: NIH; Grant number: R01 GM099766, T32 GM007270; Grant sponsors: National Institutes of Health, National Institute of General Medical Sciences; the Howard Hughes Medical Institute.

*Correspondence to: Rachel Klevit, Department of Biochemistry, University of Washington, Seattle, Washington 98195. E-mail: klevit@uw.edu or Wenqing Xu, Department of Biological Structure, University of Washington, Seattle, Washington 98195. E-mail: wxu@uw.edu
Paul A. DaRosa's current address is Department of Biology, Stanford University, Stanford, California 94305

Introduction

Tankyrase-1 and tankyrase-2 constitute two of the six members of the human poly(ADP-ribose) polymerase (PARP) enzyme family. The PARP family of proteins generate the post-translational modification poly (ADP-ribose) (PAR), a large negatively charged polymer with widespread significance for cellular functions. Protein PARylation plays important roles in a myriad of processes including DNA damage repair, cell death,[1] cell division,[2–5] and vesicle translocation.[6,7] The tankryases (TNKSs or simply tankyrase) have particularly key roles in cell growth, division, and differentiation.[8–17] As regulators of multiple signal transduction pathways including Wnt, Src, and Hippo signaling, tankyrases have emerged as important drug targets for cancer therapies.[18–20]

Other than sharing a PARP catalytic domain at its extreme C-terminus, the TNKS proteins have a unique domain composition when compared to other PARP enzymes [Fig. 1(A)]. Immediately upstream of this catalytic domain lies a SAM domain responsible for TNKSs polymerization.[21–26] The extreme N-terminal end harbors a histidine, serine, proline-rich segment (a region lacking in tankyrase-2), followed by a large ankyrin repeat domain composed of five conserved subdomains or ankyrin repeat clusters (ARCs) connected by conserved linkers. With the exception of ARC3, each ARC has a highly conserved binding groove that can recognize a tankyrase-binding motif (TBM) having the form: RXXΦDG where X is any amino acid, and Φ is a small hydrophobic amino acid (Supporting Information Fig. S1). However, considerable sequence variability is allowed at each position except the conserved Arg and Gly.[27] All confirmed tankyrase substrates to date contain one or more TBMs and it has been proposed that peptides could be utilized to block substrate binding to TNKSs as a means of a highly specific TNKS inhibition.[28]

There have been a number of reports that TNKSs can regulate the cellular concentrations of several proteins including TRF1,[11,12] 3BP2,[8,27] Axin-1/2,[9] BLF1, CASC3,[10,29] CPAP,[4] PTEN,[16] and, most recently, the angiomotin (AMOT) family of proteins,[13,14,17] in a PARylation-dependent manner. The PARylated forms of BLF1, CASC3, the disease related proteins PTEN, Axin, 3BP2, and the angiomotins are confirmed substrates of RNF146 [whose domain architecture is shown in Fig. 1(B)], which targets these proteins for degradation by attachment of poly-ubiquitin chains.[8–10,13,14,16,17]

Protein ubiquitination is a post-translational modification involved in almost all cellular processes. In general, E3 ubiquitin ligases are responsible for targeting proteins via protein-protein interactions with the substrates directly. However, RNF146 does not contain any known substrate recognition domains [Fig. 1(B)]. RNF146 was previously shown to bind the internal structural unit of the PAR polymer (known as *iso*-ADPr) via its WWE domain and RING domains.[30,31] The PAR ligand acts as an allosteric activator of the E3 ligase through a conformational change in the RING domain.[31] Hence, PAR acts as a signal for RNF146 activation. It has also been observed that RNF146 uses its C-terminal region to bind to tankyrase and that this association is required for Axin protein turnover.[31] Thus, the C-terminus of RNF146 may dictate substrate specificity or localize RNF146 with substrates through its interaction with TNKSs, allowing the E3 to target proteins PARylated by TNKSs but not other PARPs. However, the specific details of the RNF146-tankyrase interaction have not yet been investigated.

Here we show that the C-terminal fragment of RNF146 can form a one-to-one complex with the complete ankyrin repeat region of tankyrase and that several motifs within RNF146 mediate this interaction. Four of these motifs in RNF146 are noncanonical, in that they include a one or two-residue extension in the previously defined binding sequence [Fig. 1(C)]. We report the crystal structure of a noncanonical tankyrase-binding motif of RNF146 with ARC2 of mouse tankyrase-1. The structure reveals a binding mode similar to those of previous reported TBM-tankyrase interactions; but shows how an extended motif can be accommodated on the tankyrase scaffold, expanding the possible list of tankyrase substrates and interacting partners.

Results and Conclusions

RNF146 binds to tankyrases via its flexible C-terminal tail

RNF146 contains two characterized domains at its N-terminus, a RING domain and a WWE domain, which comprise the protein's ubiquitin E3 ligase activity and PAR binding function, respectively. The conserved C-terminal region of RNF146 [Supporting Information Fig. S2(A)], however, is predicted to be intrinsically disordered. Consistent with these predictions, NMR spectroscopy (^{1}H-^{15}N HSQC) of the C-terminal region of RNF146 shows a lack of ^{1}H dispersion typical of disordered proteins [Supporting Information Fig. S2(B)].

RNF146 has been reported to interact with tankyrase-1 (referred to as tankyrase or TNKS here forth) via its flexible C-terminus downstream of its WWE PAR-binding domain [see Fig. 1(B)].[31] When this region was removed no interaction with tankyrase was observed.[31] In agreement with this previous study we observe that a C-terminal fragment of RNF146 is necessary for its interaction with the substrate binding region of tankyrase (TNKS(5ARC)) via GST pull-down assays [Fig. 2(A)]. While GST-tagged RNF146 can pull-down TNKS(5ARC), a construct of RNF146 lacking the

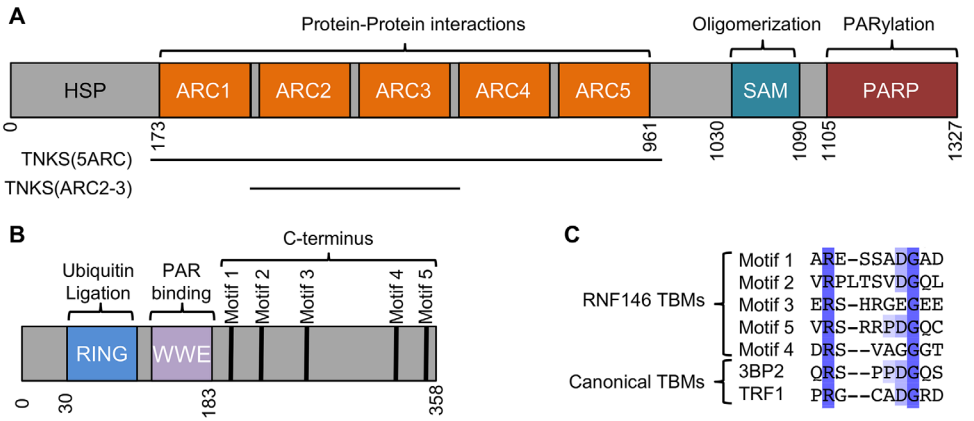

Figure 1. Domain architecture of RNF146 and Tankyrase-1/2. (A) Linear schematic of tanyrase-1/2 indicating domains and domain functions (above). Tankyrase-2 is ~83% identical to tankyrase-1, but lacks the N-terminal histidine, serine, proline rich region (HSP). (B) Linear schematic of RNF146 showing domain locations and functions. Motifs 1–5 are indicated within the disordered C-terminal domain. (C) Sequence of the TBM-like motifs in RNF146 indicated in (B). The canonical TBMs from 3BP2 and TRF1 are shown for comparison and follow the form of RXXΦDG. The symbol Φ represents any smaller hydrophic residue such as G, A, P, and V; X, any amino acid. PAR, Poly(ADP-ribose); PARylation, poly(ADP-ribosyl)ation; ARC, ankyrin repeat cluster; SAM, sterile alpha motif.

C-terminus, RNF146(ΔC-term) (residues 1–183), cannot [Fig. 2(A), lane 2 versus 1]. Furthermore, the C-terminus of RNF146 [residues 184–358; RNF146(ΔN-term)] appears to be sufficient for the RNF146-tankyrase interactions [Fig. 2(A), lane 7] despite lacking a folded protein structure. Indeed, our size exclusion chromatography (SEC) multi-angle light scattering (SEC-MALS) results demonstrate that the ΔN-term fragment of RNF146 and tankyrase form a stable one-to-one complex with a mass of 100,000 Da (± 2.55%) [Fig. 2(B) and Supporting Information Fig. S3(A)]. Therefore, the flexible C-terminal region of RNF146 is necessary and sufficient for its interaction with TNKS.

The RNF146-TNKS interaction is mediated by at least 4 motifs in the RNF146 C-terminus

Tankyrases recognize proteins via four ARC domains (ARC1, ARC2, ARC4, and ARC5) that recognize TBMs [see Fig. 1(A) and Supporting Information Fig. S1).[21] It was previously proposed that RNF146 has five motifs in its disordered C-terminus that resemble TBMs [Fig. 1(C) and Supporting Information Fig. S2(A)].[31] However, with the exception of motif 4 (RSVAGG), each TBM is one or two residues longer than previously identified TNKS binding sequences. Importantly, a mutation in motif 1, has a larger effect on tankyrase binding than motif 4, which matches the TBM consensus motif more closely.[31] That study showed that motif 1 and 4 are important for the RNF146-tankyrase interaction and that mutation of these motifs together attenuates Axin turnover in cells.[31] However, only these two motifs in RNF146 were tested previously, so we tested the remaining motifs using GST pull-down assays in which the obligate Gly in each motif is mutated to a Val residue. In agreement with the previous report,[31] motif 1 contributes to full-length RNF146 binding to TNKS(5ARC) as evident by a reduction in TNKS binding upon mutation of motif 1 [Fig. 2(A), lane 3]. Surprisingly, mutation of motifs 3 and 5 also showed that these additional motifs contribute to the interaction of RNF146 with TNKS [Fig. 2(A), lanes 3, 5, and 6]. In contrast, mutation of motif 2 does not appear to affect the interaction of RNF146 with TNKS detectably [Fig. 2(A), lane 4]. Hence, at least four of the five putative TBMs in RNF146 contribute to the RNF146-TNKS interaction despite the apparent one-residue insertion in three of the RNF146 TBMs not previously characterized as tankyrase binders.

RNF146 exhibits multivalent binding to tankyrases

The retention of binding upon mutation of specific motifs suggests a multivalent binding of RNF146 to the ankyrin repeats of TNKSs in which a number of motifs in RNF146 bind to one or more ARCs in tankyrases. To determine if RNF146 can interact with multiple tankyrase ARCs we performed pull-down experiments of individual ARC domains with each of the RNF146 motifs (motifs 1, 2, 3, 4, and 5) fused to GST [Fig. 2(C)]. In general, the individual interactions between each ARC and an isolated RNF146 TBM are much weaker than the robust binding observed for TNKS(5ARC) and full-length or RNF146(ΔN-term) as indicated by substoichiometric binding in GST pull-downs with high concentrations of protein [See Fig. 2(A,B)]. However, despite not conforming to the canonical RXXΦDG sequence (instead containing an insertion of an additional amino acid or two between the key R and G residues), all of the extended motifs show some binding to individual ARCs in tankyrase, with motif 2 only weakly binding

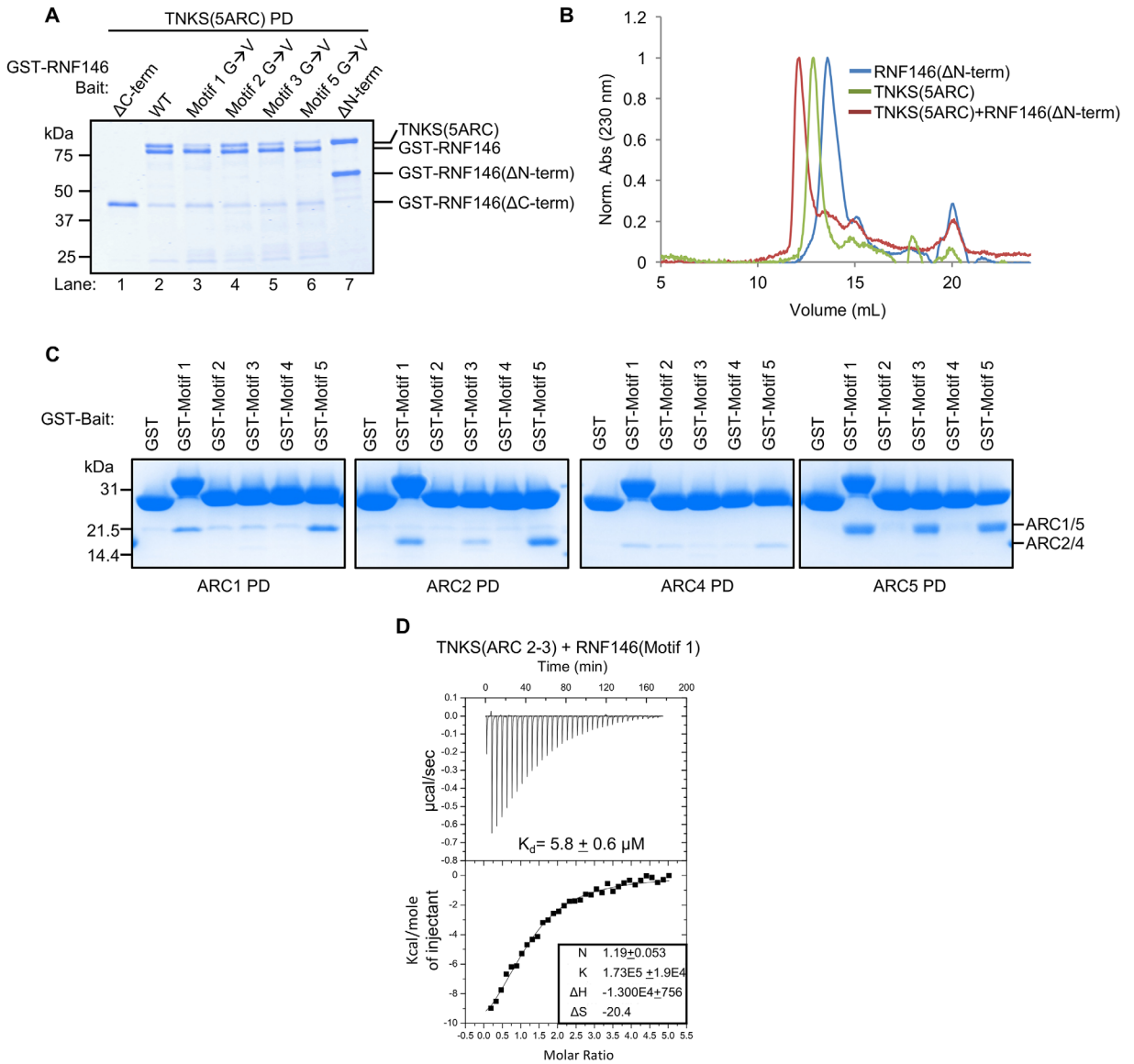

Figure 2. RNF146 binds to tankyrase via multiple motifs in its flexible C-terminus. (A) GST pull-downs of TNKS(5ARC) (residues 171–961) with GST-tagged RNF146 constructs and mutants. Mutants shown as G→V are Gly to Val mutations in the obligate Gly of the TBM. motif1 G→V, G199V; motif2 G→V, G226V; motif3 G→V, G265V; motif5 G→V, G351V; RNF146(ΔN-term), residues 184–358; RNF146(ΔC-term), residues 1–183. (B) Size exclusion chromatography (SEC) of TNKS(5ARC) (green) and RNF146(ΔN-term) (blue) and a one-to-one molar mixture of the two (red). SEC-MALS confirms a one-to-one complex of these proteins [see Supporting Information Fig. S3(A)]. (C) GST pull-downs of ARC1, ARC2, ARC4, and ARC5 with GST, or GST-RNF146 motifs 1, 2, 3, 4, or 5 with equal concentrations of starting material for each tested interaction (see Materials and Methods). (D) Isothermal titration calorimetry (ITC) of TNKS(ARC2–3) with RNF146(motif 1), showing titration curves and resulting thermodynamic parameters. A K_d of 5.8 ± 0.6 μM was measured.

to ARCs 1 and 4. Interestingly, motif 4, which is most similar to a canonical TBM, only detectibly binds ARC1 in these experiments. When individual GST-tagged ARCs are used to pull-down RNF146(ΔN-term) under the same conditions as those in Figure 2(A), only a small amount of RNF146(ΔN-term) bound to tankyrase ARCs [Supporting Information Fig. S3(B)] indicating a requirement for multiple motifs and multiple binding sites. Because motif 1 appears to have a large impact on full-length RNF146-TNKS binding [see Fig. 2(A)],[31] we measured the affinity of RNF146(motif1) for ARC2 [TNKS(ARC2-3), residues 308–655]. ITC analysis shows that the binding affinity of this interaction is 5.8 ± 0.6 μM [Fig. 2(D)], demonstrating that this extended TBM has an affinity similar to canonical TBMs (in the range of 0.3–20 μM).[27,32–34] Notably, the low affinity observed for the isolated RNF146(motif 1)-TNKS interaction supports the hypothesis that RNF146 uses multiple motifs to bind tankyrases simultaneously, because RNF146(ΔN-term) and TNKS(5ARC) (with all binding sites available) form a tight 1:1 complex that persists on a SEC

Table I. *Crystallographic Data Collection and Refinement Statistics*

TNKS(ARC2–3)/RNF146(Motif1)	PDB Code: 6CF6
Data collection	
Space group	*C121*
Cell dimensions	
a, *b*, *c* (Å)	134.02, 103.28, 75.16
α, β, γ (°)	90.0, 106.9, 90.0
Resolution (Å)	50.0–1.93 (1.98–1.93)[a]
R_{sym}(%)	5.4 (46.5)[a]
$I/\sigma I$	52.8 (2.5)[a]
Completeness (%)	97.0 (71.8)[a]
Redundancy	3.6 (2.3)[a]
Refinement	
Resolution (Å)	50.0–1.93
No. reflections	71212
R_{work}/R_{free}	19.5/22.8
No. atoms	5338
Protein	4898
Motif1 peptide	145
Water	296
B-factors	
Protein	28.4
Motif1 peptide	35.2
Water	41.9
R.M.S deviations	
Bond lengths (Å)	0.010
Bond angles (°)	1.34

This diffraction dataset was collected from a single crystal.
[a] Highest resolution shell is shown in parenthesis.
5% randomly selected reflections were used as a test set.

column [See Fig. 2(B)]. Together these data suggest that the RNF146-tankyrase interaction is mediated by multiple motifs binding to multiple ARCs simultaneously.

To test whether RNF146 requires multiple interactions at once, we performed GST pull-down assays in the presence of the competitive tankyrase interactor, Axin(1–80) (Axin, residues 1–80),[33,34] that is known to simultaneously occupy two sites on TNKSs, and we performed SEC in the presence of a large excess of RNF146. When Axin(1–80) is added as a competitor in GST pull-down assays RNF146 was competed off by a 1:1 Axin:TNKS molar ratio [Supporting Information Fig. S3(C)], indicating that competition with at most two of the TNKS sites can disrupts RNF146 binding substantially. Furthermore, when RNF146(ΔN-term) is added in a large (6 fold) excess of RNF146 in SEC experiments, RNF146 still forms a one-to-one complex with TNKS [Supporting Information Fig. S3(A, D)]. These data establish that RNF146 has multiple binding motifs that are capable of binding to multiple binding sites on tankyrases, most of which do not match the TBM consensus sequence.[27] Together and in combination with the relatively low affinity of a single TBM-ARC interaction observed, these data show multivalency in the RNF146-TNKS interaction that may be disrupted by a multivalent TNKS substrate such as Axin. Whether all TNKS substrates can displace RNF146, or if they can both weakly associate simultaneously to the ankyrin repeat region of TNKSs *in vivo* requires further investigation.

RNF146 motif 1 can bind to tankyrase-1 in a mode similar to canonical TBMs

Because the RNF146-tankyrase interaction is primarily driven by noncanonical (extended) TBMs, we sought to characterize this important protein–protein interaction structurally. We determined a crystal structure of RNF146(motif 1) (residues 184–205) in complex with TNKS(ARC2–3) at 1.93 Å resolution (Table I, Fig. 3). The overall architecture of the TNKS-RNF146 complex resembles other structures solved of TBMs bound to ARC2;[32,33] two molecules of ARC2–3 reside in the asymmetric unit forming cross pattern with a pseudo two-fold axis of symmetry resulting from an ankyrin repeat swap following the ARC2/3 helical linker (Fig. 3). One copy of the RNF146(motif 1) peptide is bound to each ARC2 module with clear electron density [Fig. 3 and Supporting Information S4(A)]. When the two sites are compared in the asymmetric unit, the two peptides have a very similar backbone conformation [Supporting Information Fig. S4(B)]. The extra residue within the RNF146 TBM is accommodated by the ARC2 binding site by diverting a three-residue segment of the main chain away from the canonical TBM trajectory [Fig. 4(A,B)].

While the length of the RNF146 TBM is longer than canonical motifs, two interaction sites are conserved in the RNF146(motif 1)-TNKS interaction. First, R193 of RNF146 falls into the conserved "arginine cradle" where hydrophobic interactions with the aliphatic chain of arginine are supplied by Trp-427, and Phe-429 interacts with the guanadinium

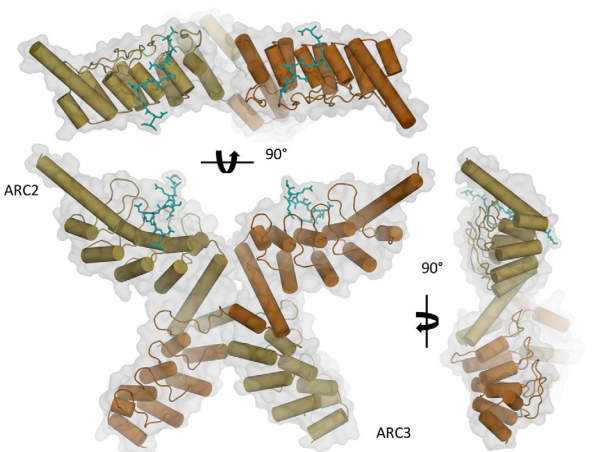

Figure 3. Structure of the RNF146(motif 1)-TNKS(ARC2–3) interaction. (A) Overall structural architecture of the RNF146(motif 1)-TNKS(ARC2–3) complex showing two copies of TNKS(ARC2–3) (yellow and orange) shown as a cartoon with helices shown as cylinders, and two peptides of RNF146(motif 1) (cyan) shown as sticks. ARC2 and ARC3 are indicated. Three angles are shown.

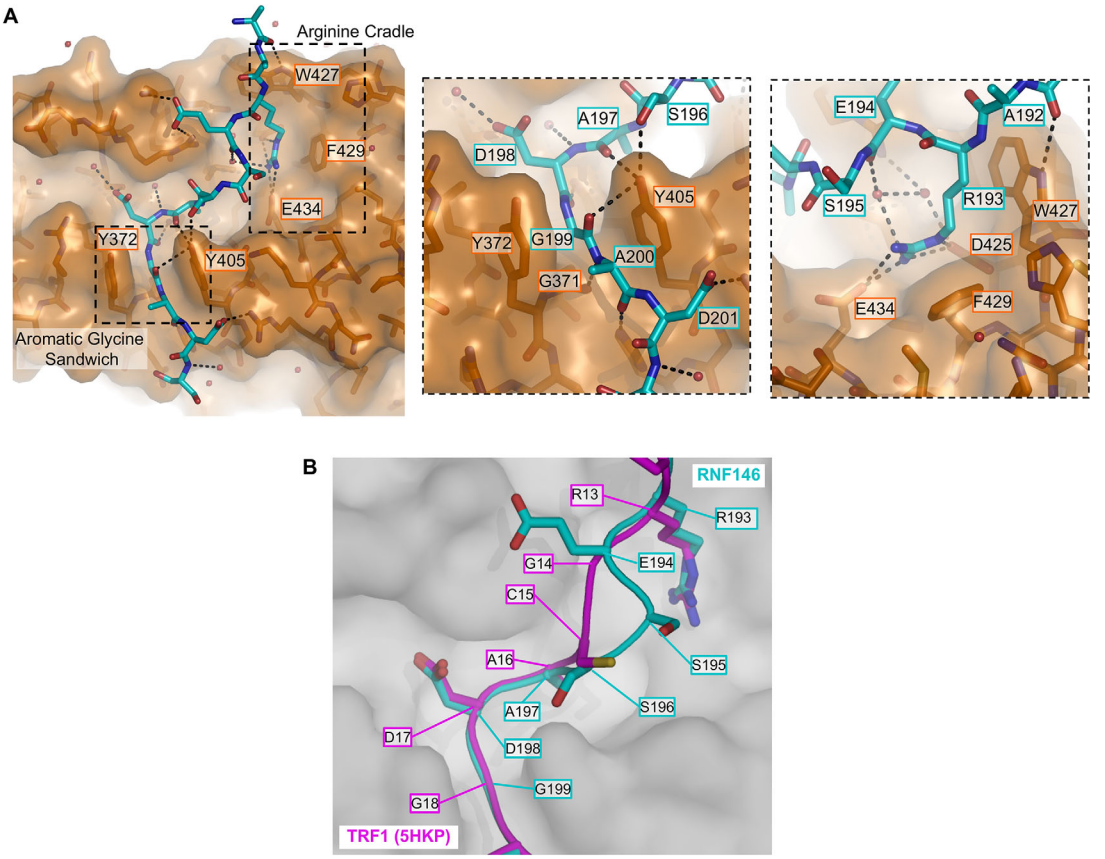

Figure 4. Determinants of RNF146 noncanonical TBM binding. (A) (*Left*) The RNF146(motif 1)-binding site on ARC2 showing the location of the arginine cradle and the aromatic glycine sandwich (dashed rectangles), and select residues. (*Middle*) A close-up of the Aromatic glycine sandwich shown in (A) and (*right*) the arginine cradle indicated in the left panel shown from an alternate angle. RNF146(motif 1) is shown as in (A), ARC2 is shown as sticks with its surface shown as orange. (B) Comparison of the peptides bound to ARC2 for RNF146(motif 1) (cyan) and TRF1 (magenta; PDB 5HKP).[32] Interactions in the arginine cradle and the aromatic glycine sandwich are maintained despite the extended RNF146 TBM. Residues are marked near their Cα atom with a line.

head group via π-stacking. TNKS Glu-434 supplies a complementary charge-charge interaction with R193 at the base of the arginine cradle [Fig. 4(A)]. Second, the "aromatic glycine sandwich" is also maintained. TNKS residues Tyr-372 and Tyr-405 form a "gate" in which only a glycine of a TBM can be accommodated [Fig. 4(A)].[27]

The greatest difference from canonical TBM-TNKS interactions falls in the central region [Fig. 4(A,B)]. The central region of RNF146(motif 1) makes a number of van der Waals interactions and hydrogen bonds, including a Tyr-carbonyl hydrogen bond previously observed between other TBM backbones and the Tyr of the ARC domain.[27,32,33] Here, this hydrogen bond is exemplified by the interaction of TNKS Tyr-405 and the backbone carbonyl of RNF146(motif 1) Ala-197 [see Fig. 4(A), center panel]. Interestingly, the extended length of the RNF146 TBM is accommodated within this central region. Relatively poor side-chain density for the Ser-195 likely indicates that this side-chain can be flexible [Supporting Information Fig. S4(C)]; there do not appear to be any protein–protein interactions at this position. Consistent with this observation, mutation of Ser-195 of the RNF146 TBM to Pro designed to disrupt the conformation of the central region of the TBM seen in the crystal structure, had no effect on RNF146(motif 1) binding in a GST pull-down experiment [Fig. 5(A)]. Also, in the central region of the TBM, the Ser-196 side-chain hydroxyl and Ala-197 main-chain carbonyl groups form a bifurcated hydrogen-bond with the Tyr-405 side-chain. However, when Ser-196 is mutated to Ala, again, there was no significant effect on GST pull-downs of ARC2 [Fig. 5(A)], consistent with the accommodation of other residues in this position of the TBM (such as the Arg found in motifs 3 and 5 at this position).

When compared with canonical TBM interactions the placement of the most conserved residues in the TBM (i.e., the obligate arginine at the N-terminus and the last four residues including the ΦDG motif) are nearly identical [Fig. 4(B)]. Therefore, the RNF146(motif 1)-TNKS interaction behaves much like a canonical TBM, where the sequence

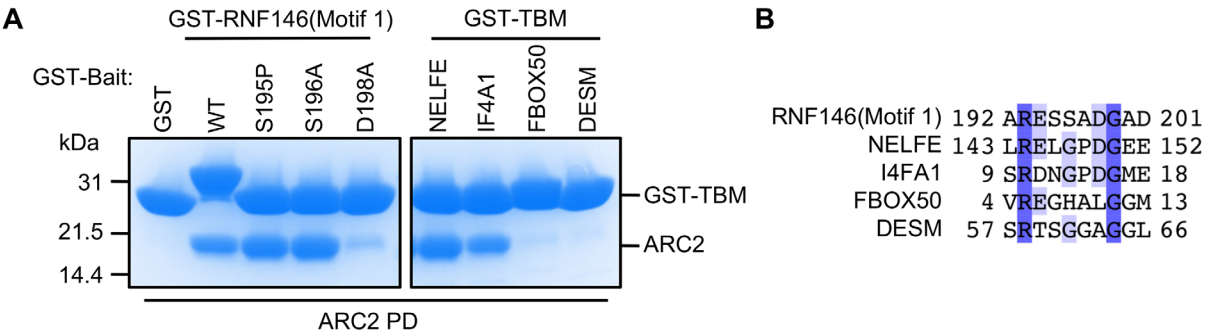

Figure 5. Extended TBMs in TNKS binding proteins. (A) GST pull-down experiments of RNF146(motif 1) WT or mutant TBMs, and extended TBMs found in NELFE, IF4A1, FBXO50, and DESM. (B) Multiple sequence alignment of RNF146(motif 1) and TBMs found in other tankyrase-binding proteins. NELFE, negative elongation factor E; IF4A1, eukaryotic initiation factor 4A-I; FBXO50, Fbox only protein 50.

rules previously established must still apply to the conserved arginine and the downstream ΦDG. Importantly, modeling the entirety of RNF146 motifs 3 and 5 based on the RNF146(motif 1)-TNKS structure suggests that these two noncanonical TBMs seen in RNF146 can be accommodated spatially in this binding mode. However, the specific interactions of residues within these motifs with the TNKSs binding sites are likely to be accommodated differently, as the residues between the conserved Gly and Arg of motif 1 are not necessarily conserved for motifs 2, 3, 4, and 5 [see Fig. 1(C)]. Still, these data open the possibility that extended TBMs may exist in other proteins.

Extended TBMs likely mediate TNKS binding to other proteins

To see if other TNKS-interacting proteins contain extended motifs we searched a list of experimentally determined tankyrase-interacting proteins determined via a tandem affinity purification followed by mass spectrometry technique.[13] Each protein in the list of 350 TNKS interactors was searched for disordered regions using the PONDR-FIT predictor.[35] The disordered regions were then searched for canonical or extended motifs with the form of RXX(A/G/P/V)XG or RXXX(A/G/P/V)XG, respectively. Within the 350 TNKS interactors, the search results returned more than 360 putative TBM motifs, including 151 extended motifs (Supporting Information Table ST1). The large number of hits returned probably reflects the simplicity of the search criteria and may contain motifs that do not form stable interactions with any of the ARCs of TNKS. However, it should be noted that, like RNF146, many tankyrase interactors may contain multiple interaction motifs. While most proteins found in our search that contain extended TBMs also contain canonical TBMs (similarly to RNF146), there are a number of proteins that only contain a single putative extended binding motif including Fbox-only protein 50 (FBXO50), desmin (DESM), negative elongation factor E (NELFE), and eukaryotic initiation factor 4A-I (IF4A1) [Fig. 5(B) and Supporting Information Table ST1). To test whether these motifs might mediate an interaction with tankyrase similar to the interaction reported here for RNF146(motif 1) and ARC2 or TNKS, we generated GST-fusions of their isolated motifs and performed pull-downs of ARC2 [Fig. 5(A)]. While no interaction was detected between ARC2 and DESM or FBXO50, the extended TBMs of IF4A1 and NELFE showed binding to ARC2 comparable to the RNF146(motif 1). Given that mutation of the Asp in the ΦDG segment of the RNF146(motif 1) results in a significant loss in binding to ARC2 [Fig. 5(A)], these data imply a preference for an acidic residue adjacent to the conserved glycine [Fig. 5(A,B)], suggesting that this residue may be particularly important for extended TBMs.

Discussion

The RNF146-TNKS interaction was previously shown to be important for Axin turnover *in vivo*.[31] Here we report the structural characterization of the fundamental recognition module of the RNF146-TNKS complex and expands on the previously known elements of this critical interaction. First, the structure of RNF146(motif 1) with ARC2 of TNKS reveals binding characteristics that are similar to well-studied TBMs and validates the TBMs of RNF146 suggested in our previous study.[31] Together with binding experiments, the structure shows how the binding motifs of RNF146 can be accommodated and bind to each of the conserved ARCs in TNKSs, and supports the hypothesis that RNF146 binds to multiple ARC domains of TNKSs simultaneously. Second, this study presents a new type of TBM that is extended by one amino acid in the middle of TBM consensus. The sequence variation in TBMs has previously been studied.[27] However, these studies focused entirely on consensus sequences with a length of four amino acids between the conserved arginine and glycine (i.e., RXXΦDG). Here we have shown the accommodation of an extra amino acid in

this motif, giving the form RXXXΦDG. This could increase the number of predicted TBMs in the proteome considerably. Indeed, our search of known TNKS binders from a recently reported dual affinity mass spectrometry screen,[13] reveals that many proteins may depend on these extended binding motifs including the confirmed binding sequences in NELFE and IF4A1. It should be noted that, while there are clearly many proteins that bind to TNKSs, little is known about which binding partners are substrates for TNKS-catalyzed PARylation, as some proteins such as GMDS can form robust interactions with TNKSs but evade modification.[36]

While our work demonstrates the basic characteristics of the RNF146-TNKS interaction, the true quaternary structure of the RNF146-TNKS interaction *in vivo* awaits further investigation. The presence of an oligomerization domain in TNKSs, known as the SAM domain, complicates our current understanding of TNKS binding. It was recently shown that the SAM domain in TNKSs can form long, helical, head-to-tail oligomers[24–26] with their N and C-termini facing away from the helical center. Hence, many TNKS ankyrin repeats will presumably be in very close proximity within larger TNKS scaffolds. Nonetheless, the one-to-one TNKS-RNF146 complex suggests that RNF146 may bind in a specific orientation that allows for substrate PARylation and subsequent ubiquitylation. Clues to such a mechanism come from a recent study on the interaction of Axin with TNKS. Axin can remodel the conformation of the TNKS(5ARC) region when it binds due to flexibility of the linkage between ARC3 and ARC4.[34] Because the C-terminus of RNF146 is highly disordered [see Supporting Information Fig. S1(A)], there are few restrictions on the access of individual RNF146 motifs within the full-length proteins. However, subtle binding preferences seen between individual TBMs of RNF146 and ARCs of TNKS may impose similar effects on the TNKS(5ARC) region as Axin, which could have direct implications on the access of RNF146 or substrates to the PARP active site.

Finally, while our crystal structure shows that the ARC2–3 fragment is present as a repeat swapped dimer similarly to previous TNKS(ARC2–3) structures,[32,33] in larger TNKS fragments such as 5ARC we do not observe dimerization in either the free TNKS(5ARC) or bound to RNF146 [see Supporting Information Fig. S3(A)]. Hence the dimerization may be a crystallographic artifact. Consistent with this we also do not observe dimerization of TNKS(5ARC) with Axin(1–80) despite ARC2–3 fragment forming a dimer in the presence of Axin(1–80).[33] Although the lack of dimerization of the TNKS(5ARC) fragment was also noted in another study,[34] we cannot not rule out the possibility that such repeat swaps do exist within oligomerized tankyrase scaffolds.

Materials and Methods

Protein expression and purification

All mouse tankyrase fragments including ARC1 (residues 171–328), ARC2 (residues 308–484), ARC4 (residues 655–800), ARC5 (residues 800–961), ARC2–3 (residues 308–655), and 5ARC (residues 171–961) were subcloned into a pGEX-4T-1 plasmid with N-terminal GST tag followed by thrombin cleavage site and an added TEV cleavage site. Full-length human RNF146 and deletions were cloned into a pGEX-6P-2 vector with an added C-terminal His_8-tag for purification. RNF146(ΔC-term) (residues 1–183) was generated by addition of a stop codon into the full-length RNF146 construct. RNF146(ΔN-term) (residues 184–358) was cloned into a pET-28a vector with His_6 and T7 tags and an added N-terminal TEV cleavage site and also cloned into pGEX-4T-1 plasmid with a GST tag and an added N-terminal TEV cleavage site. The GST-RNF146(motif 1) was generated by introducing a stop codon into the GST-RNF146(ΔN-term) construct in place of residue 206. GST-TBM constructs were generated for RNF146(motif 1) mutants (residues 191–202), RNF146 motifs 2 (residues 217–229), motif 3 (residues 257–268), motif 4 (residues 330–341), motif 5 (residues 343–355), motif 1 mutants (residues 192–203), IF4A1 (residues 7–19), DESM (residues 55–67), NELFE (residues 141–153), and FBXO50 (residues 2–13), were generated by ligating short oligonucleotides directly into the BamHI and EcoRI sites pGEX-4-T1. All other mutations were generated by site-directed mutagenesis (Stratagene) of the above constructs and confirmed by sequencing.

All proteins were produced in *Escherichia coli* (BL21(DE3)) cells in either LB media or MOPs minimal media (for RNF146(ΔN-term)), or MOPs minimal media containing ^{15}N ammonium chloride (Cambridge Isotope Labs) for ^{1}H-^{15}N HSQC experiments (NMR). Cultures were grown at 37°C to an optical density (at 600 nm) between 0.6 and 1.2, cooled to 16°C before induction with isopropyl β-D-1-thiogalactopyranoside (IPTG) (Thermo Fisher Scientific) at a final concentration of 100–400 μM. Cultures expressed overnight (ca., 16 hr) at 16°C, were spun down to pellet cells, and resuspended in 20 mM Tris pH 7.6, 200 mM NaCl, 2 mM Dithiothreitol (DTT) and frozen for future lysis. Cells were thawed at room temperature and lysed via French pressure cell press in the presence of phenylmethane sulfonyl fluoride (PMSF) (Pierce), and centrifuged at ~27,000*g* before application to affinity columns. GST-tagged ARC1, ARC2, ARC4, and ARC5 and TNKS(5ARC) were bound to Glutathione Sepherose 4B (GE Healthcare) columns, washed with five column volumes of binding buffer (20 mM Tris pH 7.6, 200 mM NaCl, 2 mM DTT) and eluted with binding buffer containing 15 mM glutathione, followed by size exclusion chromatography. Tankyrase fragments ARC2–3 and TNKS(5ARC) were similarly bound to

glutathione (GSH) beads, followed by overnight cleavage with tobacco etch virus (TEV) protease (purified as previously described)[37] on the column. After elution from Glutathione Sepherose 4B, ARC2–3 was further purified by cation-exchange chromatography (SP column; GE Healthcare) and gel filtration using a Superdex 200 column (GE Healthcare). GST-cleaved TNKS(5ARC) was then eluted from the column followed by anion exchange chromatography using a HiTrap Q HP column (GE healthcare) and size exclusion chromatography (Superdex 200; GE Healthcare). GST-tagged full-length, mutants, and truncations of RNF146 purified using Glutathione Sepherose 4B (GE Healthcare), followed by Ni-NTA (Quiagen) for affinity purification using the C-terminal His_8-tag where applicable, then anion exchange chromatography (HiTrap Q HP, GE Healthcare) and gel filtration using a Superdex 75 column (GE Healthcare). RNF146 samples prepared without a GST tag were similarly purified, but GST was cleaved using TEV protease prior to Ni-affinity purification. GST-TBM constructs were purified using glutathione sepherose 4B (GE Healthcare) affinity capture followed by elution with GST with binding buffer supplemented with 15 mM reduced glutathione followed by gel filtration. Axin(1–80) was purified as previously described.[33] The RNF146 peptide used for crystallography, residues 190–203 (NLARESSADGADS) was chemically synthesized (United Biosystems). The peptide mass was used to generate a stock solution of a known concentration in water. The concentration of peptide was confirmed by UV absorbance at 205 nm.

GST pull-down assays

GST pull-down assays using full-length GST-tagged RNF146 (or fragments or mutants thereof) shown in Figure 2(A) were performed as previously described.[31] Assays containing the competitive inhibitor Axin (residues 1–80) were performed similarly, but Axin was pre-incubated with 2 μM TNKS(5ARC) and 2 μM GST-RNF146 on ice prior to washing steps with the indicated concentrations. GST pull-down assays with GST-tagged tankyrase fragments [experiments in Supporting Information Fig. S3(B)] were performed with 1.8 nmol individual GST-ARCs and 2.5 nmol RNF146(ΔN-term), and 20 μL glutathione sepherose 4B beads. Pull-downs were performed as described above with the same volume of wash buffer and wash cycles. Individual ARC/GST-TBM pull-downs were performed as described previously [displayed in Figs. 2(C) and 5(A)].[33] In brief, 2.6 nmol of each of GST-TBM protein was added to GSH beads and incubated on ice for 30 min before washing beads three times with 200 μL of PBS binding buffer (10 mM sodium phosphate, 1.8 mM potassium phosphate, 137 mM sodium chloride, 2.8 mM potassium chloride, 2 mM DTT, and 0.1% Triton X-100) at pH 7.4. Washed beads where then incubated with 30 μL of 140 μM (4.2 nmol) of each purified (tag free) ARC domain for 1 hr on ice, and washed five times with 100 μL of PBS binding buffer. The wild type motif 1 GST-TBM construct has a larger molecular weight because of an additional TEV cleavage site upstream of motif 1 not present in the other constructs (see Protein Expression and Purification). For all pull-down experiments, protein was eluted from beads with SDS sample buffer and analyzed by SDS-PAGE.

Protein crystallization, data collection, and refinement

TNKS(ARC2–3) was buffer exchanged into 20 mM Tris pH 8.0, 100 mM NaCl, 2 mM DTT using a Superdex 200 10/300 column (GE healthcare) and concentrated to 240 μM. RNF146(motif 1) peptide (residues 190–203, NLARESSADGADS) was added to the above solution from a stock solution of 10 mM in water to give a final concentration of 1 mM peptide. One microliter of this solution was combined with 1 μL of a well solution containing 30 mM sodium citrate pH 5.6, 60 mM ammonium acetate, 27% 2-methyl-2,4-pentanediol (MPD). The TNKS(ARC2–3)/RNF146(motif 1) complex was crystalized via the hanging drop method at 4°C. Crystals formed between 2 and 3 days. Crystals were dehydrated overnight by soaking in a cryoprotectant containing 16 mM Tris pH 8.0, 80 mM NaCl, 24 mM sodium citrate pH 5.6, 48 mM ammonium acetate, 0.5 mM RNF146(motif 1) peptide, and 28% MPD before being frozen in liquid nitrogen for structure determination.

Data was collected at ALS, beamline 8.2.2. and diffraction datasets were processed using HKL2000 software package[38] with the C2 space group. The structure phase was determined by molecular replacement by searching with ARC2 and ARC3 structures from the PDB 3UTM[33] as the initial search model using Phaser,[39] followed by automated and manual model building using ARPwarp[40] and Coot.[41] The structure was refined to 1.93 Å using iterative model building using Coot and refinement using Refmac5[42] in the CCP4 7.0 software package.[43]

NMR spectroscopy

^{1}H-^{15}N HSQC-TROSY experiments were performed on a 500 MHz Bruker Avance III NMR spectrometer using ~400 μM ^{15}N labeled RNF146(ΔN-term) in 25 mM sodium phosphate pH 7.0, 150 mM NaCl, and 10% D_2O. Raw NMR data was processed using NMRpipe,[44] and analyzed in NMRviewJ (One Moon Scientific).[45]

Isothermal titration calorimetric

Isothermal titration calorimetry (ITC) was performed using a VP-ITC Microcal calorimeter (Malvern Instruments). Proteins/peptides were buffer exchanged (or resuspended) in 20 mM HEPES pH 7.5, 150 mM NaCl and degassed for ITC analysis at 20°C. Five-hundred micromolar (500 μM) RNF146(motif 1) peptide

(residues 190–203; sequence NLARESSADGADS) (United Biosystems) (titrant) was injected into 15 μM TNKS(ARC2–3) (titrand) every 5 min for a total of 40 injections at a volume of 5 μL each. Data was analyzed using the Origin 7.0 software (OriginLab Corp).

Analytical gel filtration and multi-angle light scattering

Analytical size exclusion chromatography (SEC) and SEC-MALS (multi-angle light scattering) experiments were performed using a 24 mL superdex 200 10/300 column (GE Healthcare) in a running buffer composed of 20 mM Tris pH 7.5, 150 mM NaCl, 2 mM DTT. A miniDAWN TREOS MALS detector (Wyatt Technology) was used for SEC-MALS. About 100 μg of 18 μM TNKS(5ARC) or 40 μM RNF146 was used for SEC-MALS experiments, or 100 μg TNKS(5ARC) and 50 μg RNF146(ΔN-term) for a molar excess of RNF146 for co-elution SEC-MALS experiments (final concentrations of 9 μM TNKS(5ARC) and 35 μM RNF146(ΔN-term). Prior to injection for SEC-MALS samples containing HisT7-RNF146(ΔN-term) were incubated with a very small amount of TEV protease to remove the His-T7 tag on RNF146(ΔN-term). For analytical SEC experiments only, about 100 μg of 18 μM TNKS(5ARC) were used with a large molar excess (>6 fold) of HisT7-RNF146(ΔN-term) treated with TEV protease [as seen in Supporting Information Fig. S3(D)] or about 40 μg (at 18 μM) TNKS(5ARC), 40 μg His-T7-RNF146(ΔN-term) (at 25 μM), or a 1:1 molar equivalence (final concentration of ~10 μM each) of the two proteins [as seen in Fig. 2(B)]. Ultraviolet detection of eluted proteins was monitored at 230 nm and/or 280 nm.

Disorder prediction and TBM search

A published list of tankyrase interacting proteins[13] was searched for predicted intrinsically disordered regions using the PONDR-FIT predictor.[35] The resulting predicted intrinsically disordered region (with disorder disposition scores above 0.5) were then searched using a python script for regular expression of the form RXX(A/G/P/V)XG or RXXX(A/G/P/V)XG to generate a list of potential TBMs of a canonical and an extended length (X; any amino acid).

Structure deposition information

The coordinates and structure factors for the RNF146-Tankyrase complex presented herein are available at the RCSB Protein Data Bank (PDB) with the accession code: 6CF6.

Acknowledgments

The authors thank Ning Zhang and Zhizhi Wang for advice and feedback, Brian Koepnick for writing a python script to search for regular expressions in protein sequences, and the staff of Advanced Light Source (ALS) BL 8.2.2 and the Berkeley Center for Structural Biology (BCSB) for help with data collection.

Author Contributions

P.A.D performed experiments. P.A.D., R.E.K, and W.X. conceived of experiments and wrote the manuscript.

Conflicts of Interest

The authors declare no conflicts of interest.

References

1. D'Amours D, Desnoyers S, D'Silva I, Poirier GG (1999) Poly(ADP-ribosyl)ation reactions in the regulation of nuclear functions. Biochem J 342:249–268.
2. Dynek JN, Smith S (2004) Resolution of sister telomere association is required for progression through mitosis. Science 304:97–100.
3. Chang P, Coughlin M, Mitchison TJ (2005) Tankyrase-1 polymerization of poly(ADP-ribose) is required for spindle structure and function. Nat Cell Biol 7:1133–1139.
4. Kim MK, Dudognon C, Smith S (2012) Tankyrase 1 regulates centrosome function by controlling CPAP stability. EMBO Rep 13:724–732.
5. Ozaki Y, Matsui H, Asou H, Nagamachi A, Aki D, Honda H, Yasunaga S, Takihara Y, Yamamoto T, Izumi S, Ohsugi M, Inaba T (2012) Poly-ADP ribosylation of Miki by tankyrase-1 promotes centrosome maturation. Mol Cell 47:694–706.
6. Yeh T-YJ, Sbodio JI, Tsun Z-Y, Luo B, Chi N-W (2007) Insulin-stimulated exocytosis of GLUT4 is enhanced by IRAP and its partner tankyrase. Biochem J 402:279–290.
7. Guo HL, Zhang C, Liu Q, Li Q, Lian G, Wu D, Li X, Zhang W, Shen Y, Ye Z, Lin S-Y, Lin S-C (2012) The Axin/TNKS complex interacts with KIF3A and is required for insulin-stimulated GLUT4 translocation. Cell Res 22:1246–1257.
8. Levaot N, Voytyuk O, Dimitriou I, Sircoulomb F, Chandrakumar A, Deckert M, Krzyzanowski PM, Scotter A, Gu S, Janmohamed S, Cong F, Simoncic PD, Ueki Y, La Rose J, Rottapel R (2011) Loss of tankyrase-mediated destruction of 3BP2 is the underlying pathogenic mechanism of cherubism. Cell 147:1324–1339.
9. Callow MG, Tran H, Phu L, Lau T, Lee J, Sandoval WN, Liu PS, Bheddah S, Tao J, Lill JR, Hongo J-A, Davis D, Kirkpatrick DS, Polakis P, Costa M (2011) Ubiquitin ligase RNF146 regulates tankyrase and Axin to promote Wnt signaling. PLoS One 6:e22595.
10. Zhang Y, Liu S, Mickanin C, Feng Y, Charlat O, Michaud GA, Schirle M, Shi X, Hild M, Bauer A, Myer VE, Finan PM, Porter JA, Huang S-MA, Cong F (2011) RNF146 is a poly(ADP-ribose)-directed E3 ligase that regulates axin degradation and Wnt signalling. Nat Cell Biol 13:623–629.
11. Smith S, Giriat I, Schmitt A, de Lange T (1998) Tankyrase, a poly(ADP-Ribose) polymerase at human telomeres. Science 282:1484–1487.
12. Chang W, Dynek JN, Smith S (2003) TRF1 is degraded by ubiquitin-mediated proteolysis after release from telomeres. Genes Dev 17:1328–1333.
13. Wang W, Li N, Li X, Tran MK, Han X, Chen J (2015) Tankyrase inhibitors target YAP by stabilizing angiomotin family proteins. Cell Rep 13:524–532.

14. Campbell CI, Samavarchi-Tehrani P, Barrios-Rodiles M, Datti A, Gingras A-C, Wrana JL (2016) The RNF146 and tankyrase pathway maintains the junctional Crumbs complex through regulation of angiomotin. J Cell Sci 129:3396–3411.
15. Matsumoto Y, Larose J, Kent OA, Lim M, Changoor A, Zhang L, Storozhuk Y, Mao X, Grynpas MD, Cong F, Rottapel R (2017) RANKL coordinates multiple osteoclastogenic pathways by regulating expression of ubiquitin ligase RNF146. J Clin Invest 127:1303–1315.
16. Li N, Zhang Y, Han X, Liang K, Wang J, Feng L, Wang W, Songyang Z, Lin C, Yang L, Yu Y, Chen J (2015) Poly-ADP ribosylation of PTEN by tankyrases promotes PTEN degradation and tumor growth. Genes Dev 29:157–170.
17. Wang H, Lu B, Castillo J, Zhang Y, Yang Z, McAllister G, Lindeman A, Reece-Hoyes J, Tallarico J, Russ C, Hoffman G, Xu W, Schirle M, Cong F (2016) Tankyrase inhibitor sensitizes lung cancer cells to endothelial growth factor receptor (EGFR) inhibition via stabilizing angiomotins and inhibiting YAP signaling. J Biol Chem 291:15256–15266.
18. Haikarainen T, Krauss S, Lehtio L (2014) Tankyrases: structure, function and therapeutic implications in cancer. Curr Pharm Des 20:6472–6488.
19. Lehtio L, Chi NW, Krauss S (2013) Tankyrases as drug targets. FEBS J 280:3576–3593.
20. Riffell JL, Lord CJ, Ashworth A (2012) Tankyrase-targeted therapeutics: expanding opportunities in the PARP family. Nat Rev Drug Discov 11:923–936.
21. Sbodio JI, Lodish HF, Chi N-W (2002) Tankyrase-2 oligomerizes with tankyrase-1 and binds to both TRF1 (telomere-repeat-binding factor 1) and IRAP (insulin-responsive aminopeptidase). Biochem J 361: 451–459.
22. De Rycker M, Venkatesan RN, Wei C, Price CM (2003) Vertebrate tankyrase domain structure and sterile alpha motif (SAM)-mediated multimerization. Biochem J 372:87–96.
23. De Rycker M, Price CM (2004) Tankyrase polymerization is controlled by its sterile alpha motif and poly(-ADP-ribose) polymerase domains. Mol Cell Biol 24: 9802–9812.
24. DaRosa PA, Ovchinnikov S, Xu W, Klevit RE (2016) Structural insights into SAM domain-mediated tankyrase oligomerization. Protein Sci 25:1744–1752.
25. Mariotti L, Templeton CM, Ranes M, Paracuellos P, Cronin N, Beuron F, Morris E, Guettler S (2016) Tankyrase requires SAM domain-dependent polymerization to support Wnt-β-catenin signaling. Mol Cell 63:498–513.
26. Riccio AA, McCauley M, Langelier M-F, Pascal JM (2016) Tankyrase sterile α motif domain polymerization is required for its role in Wnt signaling. Structure 24: 1573–1581.
27. Guettler S, LaRose J, Petsalaki E, Gish G, Scotter A, Pawson T, Rottapel R, Sicheri F (2011) Structural basis and sequence rules for substrate recognition by tankyrase explain the basis for cherubism disease. Cell 147: 1340–1354.
28. Xu W, Lau YH, Fischer G, Tan YS, Chattopadhyay A, De La Roche M, Hyvönen M, Verma C, Spring DR, Itzhaki LS (2017) Macrocyclized extended peptides: inhibiting the substrate-recognition domain of tankyrase. J Am Chem Soc 139:2245–2256.
29. Huang S-MA, Mishina YM, Liu S, Cheung A, Stegmeier F, Michaud GA, Charlat O, Wiellette E, Zhang Y, Wiessner S, Hild M, Shi X, Wilson CJ, Mickanin C, Myer V, Fazal A, Tomlinson R, Serluca F, Shao W, Cheng H, Shultz M, Rau C, Schirle M, Schlegl J, Ghidelli S, Fawell S, Lu C, Curtis D, Kirschner MW, Lengauer C, Finan PM, Tallarico JA, Bouwmeester T, Porter JA, Bauer A, Cong F (2009) Tankyrase inhibition stabilizes axin and antagonizes Wnt signalling. Nature 461:614–620.
30. Wang Z, Michaud GA, Cheng Z, Zhang Y, Hinds TR, Fan E, Cong F, Xu W (2012) Recognition of the iso-ADP-ribose moiety in poly(ADP-ribose) by WWE domains suggests a general mechanism for poly(ADP-ribosyl)ation-dependent ubiquitination. Genes Dev 26: 235–240.
31. DaRosa PA, Wang Z, Jiang X, Pruneda JN, Cong F, Klevit RE, Xu W (2015) Allosteric activation of the RNF146 ubiquitin ligase by a poly(ADP-ribosyl)ation signal. Nature 517:223–226.
32. Li B, Qiao R, Wang Z, Zhou W, Li X, Xu W, Rao Z (2016) Crystal structure of a tankyrase 1-telomere repeat factor 1 complex. Acta Cryst 72:320–327.
33. Morrone S, Cheng Z, Moon RT, Cong F, Xu W (2012) Crystal structure of a Tankyrase-Axin complex and its implications for Axin turnover and Tankyrase substrate recruitment. Proc Natl Acad Sci USA 109:1500–1505.
34. Eisemann T, McCauley M, Langelier M-F, Gupta K, Roy S, Van Duyne GD, Pascal JM (2016) Tankyrase-1 ankyrin repeats form an adaptable binding platform for targets of ADP-ribose modification. Structure 24: 1679–1692.
35. Xue B, Dunbrack RL, Williams RW, Dunker AK, Uversky VN (2010) PONDR-FIT: a meta-predictor of intrinsically disordered amino acids. Biochim Biophys Acta 1804:996–1010.
36. Bisht KK, Dudognon C, Chang WG, Sokol ES, Ramirez A, Smith S (2012) GDP-mannose-4,6-dehydratase is a cytosolic partner of tankyrase 1 that inhibits its poly (ADP-ribose) polymerase activity. Mol Cell Biol 32:3044–3053.
37. Tropea JE, Cherry S, Waugh DS. Expression and purification of soluble His6-tagged TEV protease. In: Doyle SA, Ed. (2009) High throughput protein expression and purification: methods and protocols. Totowa, NJ: Humana Press, pp 297–307.
38. Otwinowski Z, Minor W (1997) Processing of X-ray diffraction data collected in oscillation mode. Macromol Cryst A276:307–326.
39. McCoy AJ (2007) Solving structures of protein complexes by molecular replacement with *Phaser*. Acta Cryst 63:32–41.
40. Langer GG, Hazledine S, Wiegels T, Carolan C, Lamzin VS (2013) Visual automated macromolecular model building. Acta Cryst 69:635–641.
41. Emsley P, Lohkamp B, Scott WG, Cowtan K (2010) Features and development of Coot. Acta Cryst 66:486–501.
42. Murshudov GN, Skubak P, Lebedev AA, Pannu NS, Steiner RA, Nicholls RA, Winn MD, Long F, Vagin AA (2011) REFMAC5 for the refinement of macromolecular crystal structures. Acta Cryst 67:355–367.
43. Winn MD, Ballard CC, Cowtan KD, Dodson EJ, Emsley P, Evans PR, Keegan RM, Krissinel EB, Leslie AGW, McCoy A, McNicholas SJ, Murshudov GN, Pannu NS, Potterton EA, Powell HR, Read RJ, Vagin A, Wilson KS (2011) Overview of the CCP4 suite and current developments. Acta Cryst 67:235–242.
44. Delaglio F, Grzesiek S, Vuister GW, Zhu G, Pfeifer J, Bax A (1995) NMRPipe: a multidimensional spectral processing system based on UNIX pipes. J Biomol NMR 6:277–293.
45. Johnson BA, Blevins RA (1994) NMR view: a computer program for the visualization and analysis of NMR data. J Biomol NMR 4:603–614.